J Surfact Deterg (2010) 13:127–134
DOI 10.1007/s11743-009-1151-5

ORIGINAL ARTICLE

Interfacial Properties of Extended-Surfactant-Based Microemulsions and Related Macroemulsions

Anuradee Witthayapanyanon · Tri Thanh Phan · Todd C. Heitmann · Jeffrey H. Harwell · David A. Sabatini

Received: 9 December 2008 / Accepted: 23 April 2009 / Published online: 22 August 2009

Abstract Extended surfactants containing an intermediate-polarity spacer, such as polypropylene oxide, in between the hydrophilic head and the hydrocarbon tail are known to result in superior solubilization and low interfacial tension, though they exhibit slow kinetics. The present work seeks to evaluate both equilibrium and kinetic aspects of extended-surfactant-based micro- and macroemulsions. The interfacial morphology of the extended surfactant membrane, i.e., characteristic length (ξ) and interfacial rigidity (E_r) at optimum middle-phase microemulsion conditions, was characterized using the net-average curvature model. The results showed that extended surfactants resulted in a relatively rigid interfacial membrane compared with conventional surfactants having similar hydrocarbon chain length. In addition, both ξ and E_r parameters increased with the length of the polypropylene oxide spacer. Increasing E_r values correlated to the slow coalescence rates of extended surfactant emulsified systems. Two alternative approaches (the addition of combined linkers and co-surfactant) are shown to overcome the slow kinetics of coalescence while maintaining desirable high solubilization and low interfacial tension.

A. Witthayapanyanon · T. C. Heitmann · J. H. Harwell
Chemical, Biological, and Materials Engineering Department, Sarkeys Energy Center, University of Oklahoma, 100 East Boyd, Room T-334, Norman, OK, USA

T. T. Phan · D. A. Sabatini (✉)
Civil Engineering and Environmental Science Department, Carson Engineering Center, University of Oklahoma, 202 West Boyd, Room 334, Norman, OK 73019-1024, USA
e-mail: Sabatini@ou.edu

A. Witthayapanyanon · T. T. Phan · J. H. Harwell · D. A. Sabatini
Institute for Applied Surfactant Research, University of Oklahoma, Norman, OK 73019-1024, USA

Keywords Extended surfactants · Microemulsions · Solubilization · Characteristic length · Interfacial rigidity · Coalescence

Introduction

According to the Winsor *R*-concept [1–4], an effective way to produce microemulsions with greater solubilization and lower interfacial tension (IFT) is to equally increase the interaction of surfactant for both oil and water. While this can be achieved by increasing the hydrophilicity of the surfactant head and the length of the hydrocarbon tail, this approach is limited by the loss in solubility associated with long hydrocarbon tails. Extended surfactants have been proposed as an alternative surfactant structure to achieve the Winsor potential without sacrificing water solubility [4–7].

By definition, extended surfactants are surfactants in which intermediate-polarity groups such as short-chain polypropylene oxide (POs) or polypropylene–polyethylene oxide (POs–EOs) groups are inserted between the surfactant hydrophilic head and hydrocarbon tail [4–6]. Due to the presence of intermediate-polarity groups, extended surfactants not only increase the tail length but also offer a smoother interfacial transition from a polar aqueous to nonpolar oil region [3, 4]. As a result, extended surfactants are capable of forming middle-phase microemulsions with high solubilization and ultralow IFT for a wide range of oils, in particular long-chain alkanes, triglycerides, and vegetable oils [5–9]. Detailed discussions and proposed structures of extended surfactant can be found in the literature [3–11].

In spite of having attractive properties desirable for practical uses, extended-surfactant-based microemulsions face the challenge of poor kinetics. Our previous work [7]

reported that the equilibration time for optimum middle-phase microemulsions produced by extended surfactants is in the range of weeks to months. Such slow kinetic systems will not be adequate for application processes which operate under short contact times, e.g., detergency, hard-surface cleaning, surfactant-enhanced separation, etc.

It is widely accepted that the surfactant structure at the interface ("membrane") dictates both equilibrium and dynamic properties of microemulsion and emulsion systems [2, 12–17]. These properties include solubilization capacity, IFT reduction, phase behavior, rate of solubilization, and coalescence kinetics of macroemulsion droplets. Although many different parameters have been proposed as membrane characteristics, the present work focuses on two essential parameters: the characteristic length (ξ) and the interfacial rigidity (E_r). They are preferred because they yield vital information linked to both equilibrium and dynamic properties of microemulsion systems, as discussed further below. In addition, the net-average curvature model (NAC) [18, 19] can readily be used to estimate these membrane properties (both ξ and E_r) based on simple phase behavior and IFT data.

The characteristic length accounts for the surfactant tail plus associated oil or water molecules in the surfactant membrane, thereby determining the maximum solubilization capacity of the microemulsion system. De Gennes and Taupin [14] and Acosta et al. [18] indicated that the thickness of surfactant layer (ξ) is a function of the length parameter (L), which was later found to be an extended length scaling from the surfactant tail [18]. As for the solubilization parameter (SP), a larger value of the characteristic length suggests a higher solubilization and also results in a lower IFT. Another important property associated with the ξ parameter is the rigidity of the surfactant membrane or the interfacial rigidity (E_r). Based on a series of phase studies with linker molecules [17, 20–22], systems with higher ξ values produced a rigid surfactant membrane (high E_r values).

While ξ accounts for equilibrium microemulsion properties such as solubilization capacity and IFT, the E_r property relates to the bending modulus, K [12, 23], a key parameter controlling dynamic properties (e.g., coalescence kinetic) of microemulsion systems. Helfrich [13] proposed a mathematical equation to evaluate the K modulus in terms of the free energy required to create a new dynamic interfacial area. His work suggested that a high K-value corresponds to a rigid interfacial film, for which more energy is required to deform the membrane as two droplets approach, thereby leading to a slower coalescence rate. With this relationship, the kinetics of microemulsion equilibration may be viewed as an indirect measurement of macroemulsion coalescence rate [17], an approach which will be used in the current study as well.

Because of their unique structure, extended surfactants are likely to produce a thick and rigid interfacial membrane, which will result in a slow coalescence rate and a prolonged equilibration time. This issue is addressed in the present report after corroborating the ability of extended surfactants to form middle-phase microemulsions with desirable high solubilization and low IFT. Then, the membrane properties of the extended-surfactant-based microemulsions will be characterized using the NAC model. This information will allow comparison of interfacial thickness (ξ) and membrane rigidity (E_r) between extended surfactants and conventional surfactants having similar tail lengths. Finally, we explore approaches (i.e., the addition of combined linkers and co-surfactants) to overcome the slow coalescence rate of extended-surfactant-based systems, while still maintaining favorable low IFT and high solubilization for practical uses.

Experimental Procedures

Materials

Surfactants evaluated in this work are classified into two main groups: conventional and extended surfactants. In the first group, sodium dodecyl sulfate (SDS) and bis(2-ethylhexyl) sulfosuccinate sodium salt (SDOSS, trade name Aerosol-OT) were utilized as representatives of conventional anionic surfactants. SDS (97% active) and SDOSS (99%+) were purchased from Sigma–Aldrich. The second group of surfactants evaluated is the extended surfactants containing various numbers of propoxylated groups (PO) inserted between the sulfate head and hydrocarbon tail [R–$(PO)_x$–SO_4Na]. The hydrocarbon tail of the extended surfactants studied consisted of branched 12–13 carbons ($C_{12,13}$). These R–$(PO)_x$–SO_4Na surfactant samples were provided by Sasol North American Inc. (Lake Charles, LA); see Table 1. The 50 and 100 B indicated after the surfactant formulation represent the degree of branching of hydrocarbon tail: 50% and 100%, respectively. All conventional and extended surfactants were used as received.

Sodium chloride (99%+), *sec*-butanol (99%+, anhydrous), and straight-chain alkanes, namely octane (99%+), decane (99%+), dodecane (99%+), and hexadecane (99%+), were purchased from Sigma–Aldrich (Saint Louis, MO). Sodium mono- and dimethyl-naphthalenesulfonate (SMDNS, 99%) were supplied by Akzo Nobel (Houston, TX). All chemicals stated above were used as received.

Methods

Microemulsion phase studies were performed in flat-bottom vials with Teflon-lined screw caps using standard

Table 1 Properties of conventional and extended surfactants, and co-surfactant

Surfactants	HC	% Branch	No. of PO groups	% Active	MW	a_i (Å^2)
Conventional surfactant						
SDS	C_{12}	–	–	97.0	288	60.0[a]
SDOSS	Twin-tail C_8	–	–	100	445	110[b]
sec-butanol	C_4	–	–	>99.5	74	30.0[b]
Extended surfactants						
$C_{12,13}H_{25,27}$–$(PO)_4$–SO_4Na, 50 B	$C_{12,13}$	50	4	30.0	527	144.9[c]
$C_{12,13}H_{25,27}$–$(PO)_8$–SO_4Na, 50 B	$C_{12,13}$	50	8	30.7	766	61.73[c]
$C_{12,13}H_{25,27}$–$(PO)_8$–SO_4Na, 100 B	$C_{12,13}$	100	8	30.6	667	96.14[c]

a_i, cross-sectional area per surfactant head group

[a, b] Values reported in the literature ([34, 20], respectively)

[c] Evaluated in this work with the presence of 0.2 M NaCl addition

methods [6, 7, 20, 21]. Equal volumes of oil and water (5 mL) were added into the vial at different NaCl concentrations (salinity scan). The tubes were then placed in a temperature-controlled water bath at 27 °C. The samples were shaken once a day for the first 3 days and left to equilibrate for at least 2 weeks. When the systems reached equilibrium, the relative phase volumes and interfacial tension (IFT) values were quantified for each sample to determine the optimum condition (in this case, the salinity that produced the lowest IFT and equal volumes of oil and water solubilized in the middle phase, so that SP_o and SP_w are equal) is known as the optimum salinity (S^*) for the system.

Equilibrium interfacial tension (IFT) was measured between the excess water and excess oil phases of pre-equilibrated middle-phase microemulsion samples using a spinning drop tensiometer (University of Texas, model 500). The excess water phase of a middle-phase microemulsion (which was the dense phase) was added into the spinning drop tube. Then 1–3 μL of the excess oil phase was subsequently injected into the same tube. The IFT measurement was recorded after 15 min of spinning.

Characteristic length (ξ^*) and interfacial rigidity (E_r) of extended-surfactant-based microemulsions at the optimum condition were evaluated using the NAC approach [18], The interfacial rigidity at the optimum condition (E_r) can be calculated by the following equation [18]:

$$E_r = 4\pi\xi^{*2}\gamma^*, \quad (1)$$

where γ^* is the interfacial tension (either between middle phase and excess oil or between middle phase and excess water) at optimum condition, E_r is the interfacial rigidity expressed in k_BT units at 300 K, and ξ^* is the characteristic length at the optimum condition (Å).

Coalescence rate was estimated using the turbidity device developed by Acosta et al. [17] using a standard green light-emitting diode (LED) light source and a cadmium sulfide cell (CDS) detector. The change in the resistance was then registered via a multimeter (METEX M3850D) and converted into turbidity (τ). Coalescence samples were obtained by gently hand-shaking the optimum middle-phase microemulsions (approximate shaking rate of 20 strokes per minute) for 30 s prior to placing in the device with the light source and detector aligned at the center of the test tubes to follow the rate of macroemulsion coalescence as the equilibrium middle-phase microemulsion state is approached.

From the turbidity results, a plot of inverse turbidity ($1/\tau$) versus time (t) yields the coalescence kinetic constant (k_c) of the corresponding macroemulsion at the optimum condition.

$$\frac{1}{\tau} = k_c t + \frac{1}{\tau_0}, \quad (2)$$

where τ and τ_0 are the turbidity of samples at time t and that of the blank solution [17]. Note that Eq. 2 was established based on the assumption that a decrease in turbidity as time elapses is proportional to a decrease in the number of drops per unit volume [17]. Therefore, the k_c value indicates the rate of change of number of droplets per unit volume in the system. A higher k_c value indicates a faster coalescence of macroemulsion droplets and a quicker equilibration time toward the original middle-phase microemulsion system.

Results and Discussion

Interfacial Tension and Solubilization Properties of Extended-Surfactant-Based Microemulsions

In this study, the ability of extended surfactants to form microemulsions is compared with a conventional surfactant having a similar hydrophilic head and hydrocarbon tail.

Due to a limited number of extended surfactants available, the extended surfactant $C_{12,13}$–$(PO)_8$–SO_4Na (50% branch) and the conventional surfactant C_{12}–SO_4Na (SDS) were the closest pair available and were studied at 0.07 M concentration at 27 °C.

Figure 1 and Table 2 summarize important microemulsion properties [i.e., optimum salinity (S^*), solubilization parameter (SP^*), and interfacial tension (IFT^*)] of the $C_{12,13}$–$(PO)_8$–SO_4Na and the SDS/*sec*-butanol systems. As expected from Winsor's *R* concept [1, 2], both surfactant systems exhibit an increase in optimum salinity (S^*) with increasing oil alkane carbon number (ACN), a typical trend observed in the literature [2, 6, 7, 24]. However, it is interesting to mention that, while an increase in oil ACN results in a decrease in the minimum IFT value for the $C_{12,13}$–$(PO)_8$–SO_4Na extended surfactant, the opposite trend is observed with the SDS/*sec*-butanol system. Furthermore, according to data in Fig. 1, although the IFT^* property of $C_{12,13}$–$(PO)_8$–SO_4Na decreases with increasing oil ACN, the SP^* value remains relatively constant, an unusual behavior which deviates from the Chun Huh relationship [25, 26] which indicates that SP^* and IFT are inversely proportional.

Characteristic Length (ξ^*) and Interfacial Rigidity (E_r) of Extended Surfactant Membrane at Optimum Condition

As suggested in the introduction, with additional PO groups in the surfactant tails, extended surfactants are likely to evidence higher characteristic length (ξ^*) (thicker surfactant membrane) and more rigid surfactant membranes (E_r). Table 3 summarizes data on solubilization parameter, characteristic length, and interfacial rigidity of conventional and extended surfactant formulations for hexadecane at the optimum condition. Since the results show a consistent trend between the solubilization parameter and characteristic length, only the ξ^* value will be used as an indicator for system solubilization in later discussion. In the case of the conventional surfactant SDS and alcohol mixture, it is interesting to note that the calculated characteristic length is lower than the reported value for a usual tail length of SDS (11.64 Å versus 16 Å) [18]. The low ξ^* value indicates a weak surfactant-oil interaction which is likely the result of the high *sec*-butanol concentration and thus the low surfactant adsorption density at the interface. In respect to Eq. 1, the E_r value is strongly influenced by the ξ^* property; so the E_r value of the SDS/*sec*-butanol system is found to be very low (0.2 k_BT). A value of $E_r < 1\ k_BT$ is quite common for systems containing high amount of short-chain alcohol or hydrophilic linker [17, 18]. Furthermore, the low E_r value in the SDS/*sec*-butanol systems is also consistent with the fact that their emulsion droplets coalesced quickly after shaking ceased (≤10 min).

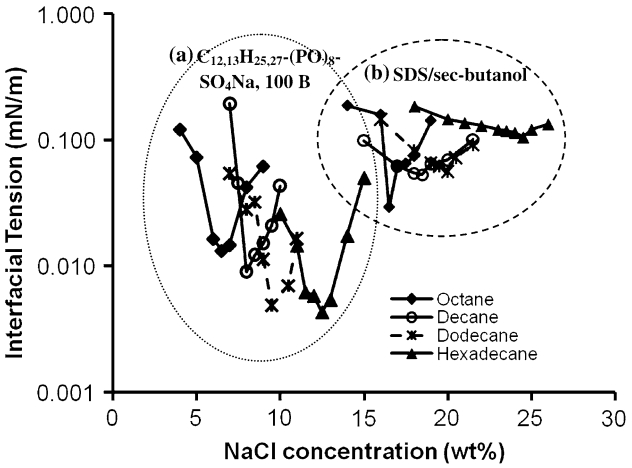

Fig. 1 Equilibrium interfacial tension (IFT) as a function of salinity of systems containing **a** $C_{12,13}H_{25,27}$–$(PO)_8$–SO_4Na, 100 B and **b** the SDS/*sec*-butanol mixture for a wide range of alkane oils at constant 0.07 M surfactant concentration and 27 °C

In contrast to the SDS/*sec*-butanol system, extended surfactant systems exhibit much higher ξ^* values (Table 3), which are a function of the number of PO groups. The results show the ξ^* value of extended surfactant notably increases from 211.8 Å to 270.1 Å on increasing the number of PO groups from four to eight. Since a higher ξ^* value means a thicker surfactant membrane and better solubilization power of microemulsion systems, this suggests that additional PO groups increase the total length of extended surfactant molecules and thus their solubilization potential.

Consistent with the ξ^* parameter, the E_r values are found to increase with increasing number of PO groups inserted into extended surfactants. The calculated E_r values for the $C_{12,13}$–$(PO)_4$–SO_4Na and $C_{12,13}$–$(PO)_8$–SO_4Na surfactants with 100% branching are 6.9 k_BT and 8.3 k_BT, respectively. From the literature [12], the E_r value for typical middle-phase microemulsion systems corresponds with the bending modulus (*K*) of 1 k_BT, whereas $E_r \approx 10\ k_BT$ suggests the presence of lipid bilayers. Based on this scale, the relatively high rigidity of the extended surfactant membrane leads to two potential explanations. First, it is possible that the extended surfactants may form a middle-phase microemulsion that coexists with liquid crystals. These liquid crystals could wrap around the emulsion droplets, inhibiting droplets from coalescing, as has been reported by others [2, 27–29]. Another potential explanation of the high-rigidity film is the steric hindrance caused by the bulky PO attachment and branch-tailed nature of extended surfactant. This effect could potentially prevent the approach of dispersed emulsion droplets or a thinning of the plane-parallel film.

Table 2 Comparison of microemulsion properties at the optimum condition between the $C_{12,13}H_{25,27}$–$(PO)_8$–SO_4Na, 100 B and the SDS/*sec*-butanol mixture for a wide range of alkane oils at constant 0.07 M surfactant concentration and 27 °C

Oil	ACN	$C_{12,13}$–$(PO)_8$–SO_4Na, 50 B			C_{12}–SO_4Na + *sec*-butanol		
		S^{*a} (wt %)	SP^{*b} (mL/g)	IFT^* (mN/m)	S^* (wt %)	SP^{*b} (mL/g)	IFT^* (mN/m)
Octane	8	6.50	6.78	0.0132	16.5	1.78	0.0292
Decane	10	8.00	5.91	0.00900	18.5	1.40	0.0528
Dodecane	12	9.50	6.26	0.00490	20.0	1.27	0.0562
Hexadecane	16	12.5	5.56	0.00430	24.5	1.01	0.105

[a] S^*, optimum salinity

[b] SP^*, total volume of middle phase (mL)/grams of surfactant

Table 3 Characteristic length (ξ^*), interfacial rigidity (E_r) at optimum conditions, and equilibration time of conventional surfactant and extended surfactant systems for hexadecane

Surfactant system	S^* (wt %)	IFT^* (mN/m)	V_{mp} (mL)	SP^{*a} (mL/g)	ξ^* (Å)	E_r (k_BT)	Equilibration time[b]
Conventional surfactant-alcohol							
SDS/*sec*-butanol	24.5	0.105	0.530	1.01	11.64	0.23	≤10 min
Extended surfactants							
$C_{12,13}H_{25,27}$–$(PO)_4$–SO_4Na, 50 B	12.8	0.0101	4.38	7.12	211.8	6.9	≈2 weeks
$C_{12,13}H_{25,27}$–$(PO)_8$–SO_4Na, 50 B	8.00	0.00750	5.70	6.53	270.1	8.3	Months

[a] SP^*, total volume of middle phase (mL)/grams of surfactants

[b] Based on visual observations of emulsified middle-phase microemulsion systems

Fish Diagram of a Single Extended Surfactant

An alternative way to present the microemulsion phase behavior is by showing a plot between surfactant concentration (M) and salinity (wt %) of the surfactant/brine/oil system. This type of plot is often portrayed in the gamma shape, thus referred to as the gamma or fish diagram [2, 10, 17].

Figure 2 is a fish diagram of the $C_{12,13}$–$(PO)_8$–SO_4Na/brine/hexadecane system. According to the diagram, the $C_{12,13}$–$(PO)_8$–SO_4Na 50B surfactant shows a vertical orientation, similar to what is typically observed for a high-purity single-component conventional anionic surfactant system. Furthermore, the fish diagram also offers two key surfactant concentrations: the critical microemulsion concentration (CμC) and the lowest surfactant concentration where a single phase (or Winsor type IV) microemulsion is formed, sometimes called the X point [2, 3, 21]. This information is highly valuable for developing a cost-effective formulation. The CμC indicates the minimum surfactant concentration required to form the "first drop" of middle-phase microemulsion and attain the lowest IFT value [6, 21], while the lowest surfactant concentration where a single phase (or Winsor type IV) microemulsion is formed guides formulators for the solubilization power of surfactant formulation [2–4]. From Fig. 2, the CμC value and the lowest point forming Winsor type IV of the $C_{12,13}$–$(PO)_8$–SO_4Na surfactant are reported as 0.37 mM (0.03 wt%) and 0.20 M (13 wt%), respectively.

Approaches to Increase the Kinetics of Coalescence with Systems Containing Extended-Surfactant-Based Microemulsions

Upon shaking the optimum system samples, the three equilibrated phases (excess oil, middle phase microemulsion, and excess water) are mixed and emulsified into a single pseudophase (macroemulsion). Since this emulsion is thermodynamically unstable, it starts to coalesce and returns to the equilibrium three-phase system as time elapses. Acosta et al. [17] used this correlation to track the kinetics of middle-phase microemulsion equilibration by measuring the turbidity of the emulsion as a function of time during coalescence (the coalescence rate). In this work, we propose that, to enhance the rate of coalescence, the rigidity of extended surfactant membrane must be reduced. Literature reports indicate that adding certain additives, such as short-chain alcohol, linkers, and branch-tailed co-surfactants, helps reduce the film rigidity (E_r) [2, 4, 14, 17, 22, 30–32]. However, whether alcohols, linkers or co-surfactants are used, they must be selected with caution since our objective is to expedite the rate of coalescence without jeopardizing the IFT and solubilization properties of microemulsion systems.

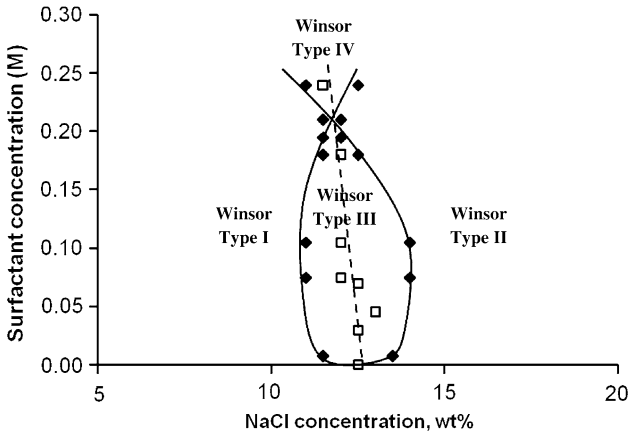

Fig. 2 *Fish diagram* of the $C_{12,13}$–$(PO)_8$–SO_4Na, 50 B/brine/hexadecane microemulsion at constant 27 °C and equal volume of oil to water

In this section, linkers and co-surfactant molecules were utilized to modify the rigidity of the extended surfactant membrane. The four extended surfactant systems evaluated were the $C_{12,13}$–$(PO)_4$–SO_4Na-alone, the $C_{12,13}$–$(PO)_4$–SO_4Na/SMDNS/dodecanol, the $C_{12,13}$–$(PO)_4$–SO_4Na–/SMDNS/oleyl alcohol, and the $C_{12,13}$–$(PO)_4$–SO_4Na/SDOSS systems, all at 27 °C. The extended surfactant $C_{12,13}$–$(PO)_4$–SO_4Na was used at constant concentration of 0.07 M unless otherwise stated. The amount of hydrophilic (SMDNS) and lipophilic linkers (dodecanol or oleyl alcohol) added was kept constant at 0.03 M. In the case of the $C_{12,13}$–$(PO)_4$–SO_4Na/SDOSS system, the total surfactant concentration was fixed at 0.07 M with a 50/50 $C_{12,13}$–$(PO)_4$–SO_4Na-to-SDOSS ratio.

Table 4 summarizes the ξ^* and E_r values of the extended surfactant and mixtures at the optimum condition. Compared with the $C_{12,13}$–$(PO)_4$–SO_4Na-alone system, the ξ^* and E_r values decrease considerably with the addition of combined linkers and the co-surfactant SDOSS, while the IFT values remain relatively constant. This result highlights that the extended surfactant is a key component in producing the low IFT property. As mentioned above, the presence of additives such as linkers or co-surfactants produces two different effects. A reduction in the ξ^* value indicates a decrease in solubilization, while a decrease in E_r value suggests a less rigid surfactant membrane, which corresponds to a faster coalescence rate (also a faster equilibration time).

Figure 3 plots inverse turbidity as a function of time during the coalescence of the emulsified system. The results show that the turbidity curve of the $C_{12,13}$–$(PO)_4$–SO_4Na surfactant alone remains relatively constant over the entire study period (total of 1 h), while the turbidity of the $C_{12,13}$–$(PO)_4$–SO_4Na mixtures drops quickly ($1/\tau$ increases rapidly) and reaches a plateau within 10 min. As noted in Eq. 2, the turbidity curve is correlated to the coalescence kinetic constant (k_c). Higher k_c values indicate a faster coalescence of macroemulsions and quick equilibration time of microemulsion systems.

Among formulations, the steepest slope (highest k_c value) is observed with the $C_{12,13}$–$(PO)_4$–SO_4Na/SMDNS/dodecanol system, while the smallest slope (smallest k_c value) is attained with the $C_{12,13}$–$(PO)_4$–SO_4Na-alone system; recall from before that higher k_c values mean greater rate of coalescence and faster approach to the equilibrium middle-phase microemulsion system. The calculated k_c values of studied systems are listed in Table 4. The $C_{12,13}$–$(PO)_4$–SO_4Na/SMDNS/dodecanol system has a k_c value three orders of magnitude higher than the $C_{12,13}$–$(PO)_4$–SO_4Na-alone system (1.2E+00 versus 4.0E-03 cm/s, respectively), indicating a faster coalescence

Table 4 Characteristic length (ξ^*), interfacial rigidity (E_r), and coalescence rate constant (k_c) of the $C_{12,13}$–$(PO)_4$–SO_4Na-alone and mixture systems at the optimum middle-phase hexadecane microemulsions and 27 °C

Surfactant system	S^* (wt %)	IFT* (mN/m)	V_{mp} (mL)	SP*[a] (mL/g)	ξ^* (Å)	E_r (k_BT)	k_c (cm/min)	Equilibration time[d]
$C_{12,13}H_{25,27}$–$(PO)_4$–SO_4Na	12.8	0.0101	4.38	7.12	211.8	6.9	4.0E-03	≈2 weeks
$C_{12,13}H_{25,27}$–$(PO)_4$–SO_4Na + SMDNS + dodecanol	17.5	0.0101	2.65	4.31	113.8	2.3	1.2E+00 ± 9.2E-02	≤10 min
$C_{12,13}H_{25,27}$–$(PO)_4$–SO_4Na + SMDNS + oleyl alcohol	16.0	0.0117	3.18	5.17	136.3	2.9	3.9E-01 ± 3.5E-04	≤10 min
$C_{12,13}H_{25,27}$–$(PO)_4$–SO_4Na + SDOSS	5.80	0.0099	1.72	2.47	96.5	1.4	3.4E-01 ± 2.3E-02[b] 2.1E+01 ± 2.3E-02[c]	≤10 min

The $C_{12,13}$–$(PO)_4$–SO_4Na concentration was fixed at 0.07 M, unless otherwise stated. The ratio of SMDNS to lipophilic linker was kept constant at 0.03 M and added on top of the 0.07 M $C_{12,13}$–$(PO)_4$–SO_4Na concentration. The ratio of $C_{12,13}$–$(PO)_4$–SO_4Na/SDOSS used was 50/50 at constant 0.07 M total surfactant concentrations

[a] SP*, total volume of middle phase (mL)/grams of surfactants

[b] The k_c value calculated from the first slope

[c] The k_c value calculated from the second slope

[d] Based on visual observations of emulsified middle-phase microemulsion systems

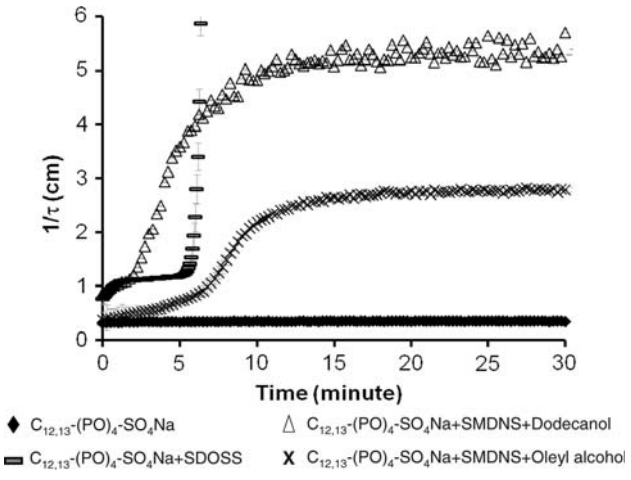

Fig. 3 The inverse turbidity curves during coalescence at 27 °C of the samples containing the 0.07 M $C_{12,13}$–$(PO)_4$–SO_4Na-alone, the 0.07 M $C_{12,13}$–$(PO)_4$–SO_4Na/0.03 M SMDNS/0.03 M dodecanol, the 0.07 M $C_{12,13}$–$(PO)_4$–SO_4Na/0.03 M SMDNS/0.03 M oleyl alcohol, and the 0.035 M $C_{12,13}$–$(PO)_4$–SO_4Na/0.035 M SDOSS mixtures. Turbidity samples resulted from shaking the optimum middle-phase hexadecane microemulsions

rate while still providing good solubilization capacity and low IFT properties. Another added benefit of the linker modified formulation is that the magnitude of solubilization power, IFT reduction, and the kinetics of coalescence can be adjusted/optimized by simply changing the type of linker molecules, as seen in the example of the $C_{12,13}$–$(PO)_4$–SO_4Na–/SDMNS/oleyl alcohol formulation.

In the case of the $C_{12,13}$–$(PO)_4$–SO_4Na/SDOSS system, the inverse turbidity plot shows a two-step increase in the $1/\tau$ value (Fig. 3), which is different from prior systems. In previous work, SDOSS was found to be much more hydrophobic than the extended surfactants [7]. By considering the difference in their hydrophilic–lipophilic nature, it is suggested that the system with $C_{12,13}$–$(PO)_4$–SO_4Na and SDOSS may produce two different types of surfactant membranes or may transition over time in the composition at the interface, with the high ratio of SDOSS to $C_{12,13}$–$(PO)_4$–SO_4Na exhibiting different properties than the high fraction of $C_{12,13}$–$(PO)_4$–SO_4Na at the interface. In Table 4, two distinctive k_c values are calculated from the individual slopes in the $C_{12,13}$–$(PO)_4$–SO_4Na/SDOSS system. In addition, although the bicontinuous middle phase (MP) might tend to be the continuous phase in macroemulsion systems, given the disproportionate volumes between the MP and excess oil and water phases, this MP phase could also be a dispersed phase in some cases. Therefore, the case of the Winsor III microemulsion possibly consists of the coalescence of multiple emulsion systems (e.g., O/W, W/O, O/MP, and W/MP), and the coalescence rates are slowest for systems containing the MP as a continuous phase [15, 33]. Regarding this fact, it is possible that the $C_{12,13}$–$(PO)_4$–SO_4Na/SDOSS system may produce multiple emulsions. Further study is required to gain improved understanding of this mixture behavior. Nonetheless, from a practical perspective, the equilibration time is $\leq$10 min as compared with 2 weeks for the extended surfactant alone, thereby again illustrating the ability of this co-surfactant to improve the system's kinetics.

Acknowledgments Funding for this research was provided by industrial sponsors of the Institute for Applied Surfactant Research at University of Oklahoma: Akzo Nobel, Clorox, Conoco-Philips, Church and Dwight, Dow Chemical, Ecolab, Halliburton, Huntsman, Oxiteno, Procter & Gamble, Sasol North America, S.C. Johnson & Son, and Shell Chemical. The authors would like to express their gratitude to Geoff Russell and Victoria Stolarski, Sasol North America (Lake Charles, LA) for providing extended surfactant samples. Final thanks go to Prof. Jean-Louis Salager and Dr. Antonio Cardenas for useful discussions and literature suggestion.

References

1. Winsor PA (1948) Solvent properties of amphiphilic compounds. Trans Faradays Soc 44:736
2. Bourrel M, Schecter R (1988) Microemulsions and related systems. Marcel Dekker, New York
3. Salager JL (1999) Microemulsions. In: Broze G (ed) Handbook of detergents: part A: properties. Marcel Dekker, New York, pp 253–302
4. Salager JL, Anton RE, Sabatini DA, Harwell JH, Acosta EJ, Tolosa LI (2005) Enhancing solubilization in microemulsions—state of the art and current trends. J Surfactant Deterg 8(1): 3–21
5. Miñana-Pérez M, Graciaa A, Lachaise J, Salager JL (1995) Solubilization of polar oils with extended surfactants. Colloid Surf A 100:217–224
6. Witthayapanyanon A, Acosta EJ, Harwell JH, Sabatini DA (2006) Formulation of ultralow interfacial tension systems using extended surfactants. J Surfactant Deterg 9(4):331–339
7. Witthayapanyanon A, Harwell JH, Sabatini DA (2008) Hydrophilic-lipophilic deviation (HLD) method for characterizing conventional and extended surfactants. J Colloid Interface Sci 325:259–266
8. Yanatatsaneejit U, Rangsunvigit P, Scamehorn JF, Chavadej S (2005) Removal by froth flotation under low interfacial tension conditions I: foam characteristics, coalescence time, and equilibrium time. Sep Sci Technol 40:1537
9. Childs J, Acosta EJ, Scamehorn JF, Sabatini DA (2005) Surfactant-enhanced treatment of oil-based drilling cuttings. J Energy Res Technol 127:153–162
10. Do L, Witthayapanyanon A, Harwell JH, Sabatini DA (2009) Environmentally friendly vegetable oil microemulsions using extended-surfactants and linkers. J Surfactant Deterg 12:91–99
11. Salager JL, Scorzza C, Forgiarini A, Arandia MA, Pietrangeli G, Manchego L, Vejar F (2008) Amphiphilic mixtures versus surfactant structures with smooth polarity transition across interface to improve solubilization performance. 7th World Surfactant Congress, Paris, France
12. Microemulsions http://www.chm.bris.ac.uk/eastoe/surf_Chem/3%20Microemulsions.pdf
13. Helfrich WZ (1973) Elastic properties of lipid bilayers: theory and possible experiments. Naturforsch 28C:693

14. De Gennes PG, Taupin C (1982) Microemulsions and the flexibility of oil/water interfaces. J Phys Chem 86:2294–2304
15. Binks BP (1998) Emulsions-recent advances in understanding. In: Binks BP (ed) Modern aspects of emulsion science. Royal Society of Chemistry, Great Britain, pp 1–55
16. Carroll BJ (1981) The kinetics of solubilization of nonpolar oils by nonionic surfactant solutions. J Colloid Interface Sci 79:126–135
17. Acosta EJ, Le MA, Harwell JH, Sabatini DA (2003) Coalescence and solubilization kinetics in linker-modified microemulsions and related systems. Langmuir 19:566–574
18. Acosta EJ, Szekeres E, Harwell JH, Sabatini DA (2003) Net-average curvature model for solubilization and supersolubilization in surfactant microemulsions. Langmuir 19:186–195
19. Acosta E (2004) Modeling and formulation of microemulsions: the net-average curvature model and the combined linker effect. Dissertation, University of Oklahoma
20. Acosta E, Mai PD, Harwell JH, Sabatini DA (2003) Linker-modified microemulsions for a variety of oils and surfactants. J Surfactant Deterg 6(4):353–363
21. Acosta EJ, Harwell JH, Sabatini DA (2004) Self-assembly in linker-modified microemulsions. J Colloid Interface Sci 274:652–664
22. Sabatini DA, Acosta E, Harwell JH (2003) Linker molecules in surfactant mixtures. Curr Opin Colloid Interface Sci 8:316–326
23. Langevin D, Meunier J (1994) Interfacial tension: theory and experiment. In: Gelbart WM, Ben-Shaul A, Roux D (eds) Micelles, membranes, microemulsions and monolayers. Springer-Verlag, New York
24. Miñana-Pérez M, Graciaa A, Lachaise J, Salager JL (1995) Solubilization of polar oils in microemulsion systems. Progr Colloid Polym Sci 98:177–179
25. Huh C (1979) Interfacial tension and solubilizing ability of a microemulsion phase that coexists with oil and brine. J Colloid Interface Sci 71:409
26. Huh C (1983) Equilibrium of microemulsion that coexist with the oil and brine. Soc Pet Eng J 23:829
27. Tolosa LI, Forgiarini A, Moreno P, Salager JL (2006) Combined effects of formulation and stirring on emulsion drop size in the vicinity of three-phase behavior of surfactant-oil-water systems. Ind Eng Chem Res 45:3810–3814
28. Wasan DT, McNamara JJ, Shaw SM, Sampath K, Aderangi N (1979) The role of coalescence phenomena and interfacial rheological properties in enhanced oil recovery: an overview. J Rheol 23(2):181–207
29. Flumerfelt RW, Catalano AB, Tong CH (1981) The coalescence characteristics of low tension oil-water-surfactant systems. Proceeding of Symposium on Surface Phenomena for Enhanced Oil recovery, pp 571
30. Kazlov MM, Helfrich W (1992) Effects of a cosurfactant on the stretching and bending elasticities of a surfactant monolayer. Langmuir 8:2792–2797
31. Gradzielski M (1998) Effect of the cosurfactant structure on the bending elasticity in nonionic oil-in-water microemulsions. Langmuir 14:6037–6044
32. Meglio JM, Dvolaitzky M, Taupin C (1985) Determination of the rigidity constant of the amphiphilic film in birefringent microemulsions: the role of the cosurfactant. J Phys Chem 89:871–874
33. Hazlett RD, Schecter RS (1988) Stability of macroemulsions. Colloids Surf 29:53–69
34. Rosen MJ (2004) Surfactants and interfacial phenomena. Wiley, New Jersey

Author Biographies

Anuradee (Oat) Witthayapanyanon received her BS (2001) in Chemical Engineering from the King Mongkut University of Technology Thonburi, Thailand. In 2003, she obtained her MS in Petrochemical Technology from Chulalongkorn University, Thailand. She recently received her PhD in Chemical Engineering from the University of Oklahoma (2008). Her dissertation focused on a novel study of extended surfactants in microemulsion formation.

Tri Thanh Phan received his BS (1996) in Chemical Engineering from the Polytechnic University of Ho Ci Minh City, Vietnam and his MS in Environmental Engineering from the Asian Institute of Technology, Thailand in 2001. He is currently a PhD candidate at the Department of Civil Engineering and Environmental Science.

Todd C. Heitmann is a junior undergraduate student at the School of Chemical, Biological, and Materials Engineering at the University of Oklahoma. He has been involved in the undergraduate research program as a laboratory assistant under the supervision of Dr. David A. Sabatini since 2007. He is expected to complete his BS in the spring of 2010.

Jeffrey H. Harwell is a Conoco/DuPont and George Lynn Cross Research Professor of Chemical, Biological, and Materials Engineering at the University of Oklahoma. He received his BA (1974) and MS (1979) from Texas A&M University and his PhD (1983) from the University of Texas at Austin. His research ranges from fundamental surfactant study such as novel microemulsion formation to applied areas such as environmental remediation, cleaning formulations, and nanotechnology.

David A. Sabatini David Ross Boyd Professor and Sun Oil Company Chair of Civil Engineering and Environmental Science, is an Associate Director of the Institute of Applied Surfactant Research at the University of Oklahoma. He received his BS from the University of Illinois (1981), his MS from Memphis State University (1985), and his PhD from Iowa State University (1989). His research focuses on surfactant-based subsurface remediation, surfactant-based formulations for vegetable oil extraction and biodiesel applications, and advanced microemulsions for cleaning systems.